JOURNAL OF GUIDANCE, CONTROL, AND DYNAMICS
Vol. 30, No. 4, July–August 2007

High-Precision, Symplectic Numerical, Relative Orbit Propagation

E. İmre* and P. L. Palmer†
Surrey Space Centre, University of Surrey, Guildford, GU2 7XH, UK

DOI: 10.2514/1.26846

This paper presents a numerical method to propagate relative orbits. It can handle an arbitrary number of zonal and tesseral terms in the geopotential. This method relies on defining a *relative Hamiltonian*, which describes both the absolute and the relative motion of two satellites. The solution is separated into an analytical Keplerian part and a symplectic numerical integration part. The algorithm is designed to conserve the constants of the motion, resulting in better long-term accuracy. We present results for a broad range of scenarios with large separations and show that submeter accuracy is possible over five days of propagation, with a geopotential model containing 36 terms in tesseral and zonal harmonics. These results are valid for eccentricities reaching 0.5. Furthermore, the relative propagation scheme is significantly faster than differencing two absolute orbit propagations.

I. Introduction

MODELING the relative motion between two satellites requires computing the orbital motion of each and differencing them. Analytic models provide greater insight into the variation of relative positioning, but they rapidly become very complex as they incorporate various effects, all of which are of equal importance. The approach we propose here is to use a numerical integration of explicit relative motion equations. Such an approach allows a wide range of perturbing effects to be included. We will first review the development of analytic models before considering numerical approaches to this problem.

Analytic models of relative motion usually start from Clohessy–Wiltshire (CW) [1] or Hill equations [2], which are the linearized Keplerian relative motion equations for near-circular orbits. This model has been employed successfully for a short-term rendezvous type of mission.

Various methods have been proposed to extend this near-circular Keplerian solution to include the effects of J_2 [3–8], eccentricity [9–13], and atmospheric drag [14]. There have also been some attempts to incorporate higher-order potential terms into the solution, but with eccentricity limitations [15–18]. Karlgaard and Lutze [19] derived second-order solutions to the Keplerian relative motion equations for use with formation flying of satellites on circular orbits.

Most of these analytic models all use a local rotating coordinate frame. Although this approach makes the analysis of the unperturbed motion very straightforward, the addition of perturbation terms in the force calculation are made significantly more complex. For this reason, models incorporating the effects of J_2 rapidly become quite unwieldy. Recently, Melton [20] and Alfriend and Han [21] published evaluations of different approaches for the analytical modeling of the relative motion, the latter via an error index that they define. They show that, not surprisingly, J_2-inclusive nonlinear models provide much better long-term accuracy than their Keplerian-only counterparts and CW equations have difficulty handling even very small (10^{-3} level) eccentricities. This underlines the importance of employing better models of the gravitational potential.

Our previous work [22] focused upon a simple linearized analytical expression for the Keplerian relative motion without restriction to orbital eccentricity. The approach was different from other approaches in that our starting point was not the near-circular case and no rotating frame was employed. The method was based upon the derivation of a relative Hamiltonian that preserved strictly conserved quantities in the full Keplerian problem: the differences in orbital energy and orbital angular momenta. We demonstrated how to set initial conditions to accurately reflect these conserved quantities and thus obtain a much higher degree of accuracy in the description of relative motion over extended time scales. Even when J_2 is included, the relative motion should conserve relative energy and the z component of the angular-momentum difference.

The literature on numerical relative orbit propagation, on the other hand, is virtually nonexistent. One interesting exception is Encke's method (as cited by Bate et al. [23]), which is originally used for the numerical integration of perturbed orbits, in which the perturbations to the Keplerian orbit are integrated numerically.

Navigation in space is carried out via combining measurements from sensors with a mathematical model of the motion, within a filter to smooth out the data. High-precision relative navigation sensors [e.g., carrier-difference global positioning system (CDGPS) or laser] usually require large amounts of power and/or computational resources. For example, Busse et al. [24] (see also Inalhan et al. [25]) recently published a complete relative navigation solution via an adaptive extended Kalman filter. They use a simple linear Keplerian dynamic model, and this needs to be supplemented with accurate CDGPS sensor data at a rate of 1 Hz, which means that GPS has to be kept on all the time. On the other hand, it is desirable to turn these systems on as infrequently as possible, particularly in view of the fact that one of the aims of formation flying is to distribute the workload and make the individual satellites smaller with limited resources. There is, therefore, an advantage in employing a more accurate mathematical model of the motion, because this requires fewer samples to be made with the sensor.

This paper describes the derivation of a novel symplectic numerical, relative orbit-propagation algorithm that can accommodate not only the primary Earth oblateness term J_2, but also an arbitrary number of higher-order geopotential terms. The method is designed to strictly conserve all quantities invariant to the motion and is fast, for working within a Kalman style filter. Other perturbation terms, such as atmospheric drag, can be easily incorporated (such as by extending the method by Malhotra [26]), although these will not be described here.

II. Modeling of the Motion

The motion of a satellite orbiting a planet cannot be completely described by a Keplerian orbit, particularly if at a low altitude. The analytic solution of Keplerian motion is a useful approximation, but will produce positional errors on the order of a few kilometers in the case of an Earth-orbiting satellite. When considering the motion of

Received 27 July 2006; revision received 25 January 2007; accepted for publication 30 January 2007.

*Currently Senior Researcher, Ph.D., TÜBİTAK-UZAY Space Research Institute, 06531 Ankara, Turkey; egemen.imre@uzay.tubitak.gov.tr.

†University Reader. Member AIAA.

multiple satellites in close proximity, such errors are unacceptably large (at least as large as, if not larger than, their separations). As a consequence, a more accurate orbit model is required for the motions of these satellites, and this means that a numerical solution to the equations of motion can be extremely useful.

Numerical solutions to satellite motion can be made significantly more accurate than the analytic models by incorporating higher numbers of terms in the gravitational potential, expressed as an infinite series of spherical harmonics. To propagate the orbit of a satellite, usually around 40 zonal terms for the Earth are employed, because this provides an adequate description to typical machine accuracy [27].

A number of accurate numerical schemes have been devised to propagate satellite trajectories. Montenbruck [28] describes many of them, such as the Runge–Kutta methods, multistep methods (e.g., Stoermer–Cowell and Adams–Bashforth) and extrapolation methods (Bulirsch–Stoer); see also Palmer et al. [29] for a comparison of different methods.

Recent advances in this field have seen the introduction of symplectic methods [30–35]. These methods are geometric integrators, which means that they preserve, to high precision, the constants associated with the motion. In the case of satellite orbits, this means that the orbital energy and components of angular momentum are strictly conserved, as dictated by the real dynamics of the problem. These geometric properties stem from the Hamiltonian description of the motion and its consequent area-preserving quality in phase space. The advantage of exploiting these symplectic properties is that the integrators are much faster for the same level of accuracy than their nongeometric counterparts such as Bulirsch–Stoer. This is because by preserving the geometry and employing more efficient integration of forces of different magnitudes, larger time steps may be used than with those of the other methods.

When using such numerically propagated solutions for formation flying, however, we need to know the relative positions and velocities between satellites, and this means subtracting two almost identical large values to measure a small difference. This greatly magnifies the error in the description of the relative motions between the satellites, particularly for onboard applications with limited numerical precision. In addition, significant gains in computational time can be had without large penalties in relative positioning error. Therefore, we would like to be able to propagate the relative motion directly. If we are to exploit the success of symplectic propagation methods, then the description of relative motion needs to completely preserve relative energy differences and angular-momentum differences. We therefore seek a method of describing relative motion in terms of a Hamiltonian system.

A. Description of Motion in Inertial Space

We start by considering the motion of a single satellite in inertial space, orbiting around a planet. The motion of the satellite can be described using the Hamiltonian:

$$H(\mathbf{r},\mathbf{v}) = K + R = \frac{1}{2}v^2 - \frac{\mu}{r} + R(\mathbf{r}) \tag{1}$$

where $K = K(\mathbf{r},\mathbf{v})$ is the Hamiltonian describing Keplerian motion, R is the perturbing function due to the remaining terms in the spherical harmonic expansion of the gravitational field of the planet, and μ is the gravitational parameter (GM, where M is the mass of the planet). We can write R explicitly as

$$R(r,\varphi,\theta) = \frac{\mu}{r}\sum_{n=2}^{N}\sum_{m=0}^{n}\left(\frac{R_\oplus}{r}\right)^n P_n^m(\cos\theta)[C_{nm}\cos m\varphi + S_{nm}\sin m\varphi] \tag{2}$$

where (r,φ,θ) are spherical polar coordinates fixed in the Earth, measured from the rotation axis [27].

From this Hamiltonian, the equations of orbital motion can be derived. The symplectic approach exploits the exact analytic solution of the Keplerian motion and the fact that R is much smaller than K in magnitude. In the case of the Earth, R is about 10^3 times smaller. In the leapfrog scheme, the propagation of satellite position and velocity proceeds by first propagating the motion over half a time step, ignoring the R term completely. This is followed by a propagation ignoring K completely over a full time step. Because R is independent of velocity, this causes a jump in velocity with no change of position:

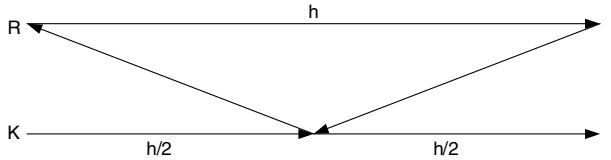

Fig. 1 Basic leapfrog algorithm.

$$\Delta\mathbf{v} = -h\frac{\partial R}{\partial \mathbf{r}} \tag{3}$$

Then comes another half-time-step evolution ignoring R, using the updated velocity [36]; this is shown in Fig. 1.

The reason this approach works so well is because at each step of the procedure, the error has a Hamiltonian form. This causes the energy to oscillate but it never diverges; therefore, even for reasonably large time steps, the energy is conserved. As the time step continues to increase, the system starts to become chaotic and the stability of the method collapses [34].

As already shown, the Hamiltonian can be written as a sum of two Hamiltonians, such as $H = K + R$. If the time step is h, then we can express this procedure in a symbolic form using Lie operators [37]. The preceding leapfrog scheme is then

$$\exp\left(\tfrac{1}{2}hK\right)\exp(hR)\exp\left(\tfrac{1}{2}hK\right) \tag{4}$$

The Lie operator $\hat{H}$ gives the time derivative of an arbitrary function $f(p,q,t)$ (with p and q being canonical variables), which is moving under a Hamiltonian H (i.e., $\dot{f} = f\hat{H}$ [37]). This can be used to describe how this function moves forward in time, under the motion defined by this Hamiltonian, with the notation $\exp(h\hat{H})f(p,q,0) = f(p,q,h)$.

There is a direct relationship between symplectic methods and conventional integration schemes that allows for higher-order schemes to be developed [38]. Using this, we can derive higher-order symplectic schemes that involve more force evaluations per step but reduce the order of the error in terms of the time step. A balance can be struck between increasing the time step using higher-order schemes and the increasing overhead of more force evaluations per step. We have found that it is best using a sixth-order scheme for the largest components of the acceleration, whereas higher-order terms in R may be evaluated using lower-order schemes. Section III.A contains a more in-depth discussion of how these higher-order schemes are constructed.

B. Hamiltonian Description of Keplerian Relative Motion

In this section, we shall consider the relative motion between two satellites moving in a Keplerian potential, focusing on the conserved quantities of the motion. Because a substantially more detailed treatment was presented in our previous work [22], we will limit ourselves to a brief summary here.

We start by considering a satellite at position $\mathbf{r}$ moving with velocity $\mathbf{v}$ in a Keplerian potential. The Hamiltonian for this satellite is given by

$$H = \frac{1}{2}(\mathbf{v}\cdot\mathbf{v}) - \frac{\mu}{r} \tag{5}$$

where μ is the gravitational parameter defining the potential. The position and velocity of this satellite defines coordinates in a six-dimensional phase space, and Hamilton's equations define the motion of the satellite through this phase space at all later times. Now

suppose that instead of a single satellite there are two satellites in close proximity to each other in this phase space. We can define the position and velocity of these two satellites as $\mathbf{r} \pm \delta\mathbf{r}$ and $\mathbf{v} \pm \delta\mathbf{v}$. This description locates the midpoint in phase space as defined by $\mathbf{r}$ and $\mathbf{v}$ and the deviation from this midpoint for each of the two satellites. Consider the Hamiltonian that describes the motion of the satellite for which the small increments in phase-space coordinates are added to the midpoint coordinates:

$$H_1 = \frac{1}{2}(\mathbf{v}\cdot\mathbf{v}) + \frac{1}{2}(\mathbf{v}\cdot\delta\mathbf{v}) - \frac{\mu}{r}\left[1 - \frac{1}{2}\frac{\mathbf{r}\cdot\delta\mathbf{r}}{\mathbf{r}\cdot\mathbf{r}}\right] \tag{6}$$

The Hamiltonian for the second satellite (H_2) can be found from the preceding by reversing the signs of $\delta\mathbf{r}$ and $\delta\mathbf{v}$. According to the theory of Hamiltonian systems, both of these quantities are conserved by the motion. We would therefore like to find a description of the relative motion that also conserves these quantities and exploits the fact that the separations in phase space are small.

The relative energy is defined as the difference between the following two Hamiltonians:

$$H_R = H_1 - H_2 = \mathbf{v}\cdot\delta\mathbf{v} + \frac{\mu}{r^3}(\mathbf{r}\cdot\delta\mathbf{r}) \tag{7}$$

The important point to note in this expression is that by our choice of describing the motion in terms of the phase-space midpoint, the second-order terms in H_R cancel. Hence, the relative energy is accurate to third order. Furthermore, we will shortly exploit this midpoint definition to greatly increase the accuracy of our relative propagation scheme.

We can think of the relative motion of the two satellites as a motion in a 12-dimensional phase space defined by the position and velocity of the midpoint and the separation positions and velocities. In this context, we may generalize the set of Hamilton's equations to obtain the following set in 12 dimensions:

$$\dot{\mathbf{r}} = \frac{\partial H_R}{\partial \delta\mathbf{v}} \qquad \dot{\mathbf{v}} = -\frac{\partial H_R}{\partial \delta\mathbf{r}} = -\frac{\mu}{r^3}\mathbf{r} \tag{8}$$

$$\delta\dot{\mathbf{r}} = \frac{\partial H_R}{\partial \mathbf{v}} \qquad \delta\dot{\mathbf{v}} = -\frac{\partial H_R}{\partial \mathbf{r}} = -\frac{\mu}{r^3}\delta\mathbf{r} + \frac{3\mu}{r^5}(\mathbf{r}\cdot\delta\mathbf{r})\mathbf{r} \tag{9}$$

These equations are an extension of the Hamilton's equations in six dimensions, but there is a cross-coupling between the relative motion and absolute motion of the midpoint. The acceleration in Eq. (8) shows that the motion of the midpoint reduces to Keplerian motion. Equation (9), on the other hand, describes the relative motion.

Similarly, writing the angular momentum for two satellites and taking the difference, one can obtain the relative angular momentum L_R. Hence, the Keplerian relative motion solution presented in [22] is called the $H_R L_R$ method. It is straightforward to show that both H_R and L_R are conserved quantities.

C. Relative Motion with Perturbations

In the previous section, we showed that the equations of motion can be written for the relative motion in a Keplerian potential using the Hamiltonian description. We will now generalize this method for a geopotential with an arbitrary number of terms in the spherical harmonics. For this, we introduce the total gravitational potential $U(\mathbf{r})$, such that

$$U(\mathbf{r}) = -\frac{\mu}{r} + R(\mathbf{r}) \tag{10}$$

The Hamiltonian for a single satellite was given in Eq. (1). In a similar fashion, we can generalize Eq. (6) as

$$H_1 = \tfrac{1}{2}(\mathbf{v} + \tfrac{1}{2}\delta\mathbf{v})\cdot(\mathbf{v} + \tfrac{1}{2}\delta\mathbf{v}) + U(\mathbf{r} + \tfrac{1}{2}\delta\mathbf{r}) \tag{11}$$

Because our satellites are moving in close proximity to each other, we may expand the potential functions in a Taylor series about the midpoint location $\mathbf{r}$. Ignoring terms $\mathcal{O}(\delta\mathbf{r}^3)$ the Hamiltonian becomes

$$H_1 = \frac{1}{2}\left[\mathbf{v}\cdot\mathbf{v} + (\mathbf{v}\cdot\delta\mathbf{v}) + \frac{1}{4}(\delta\mathbf{v}\cdot\delta\mathbf{v})\right] + \left[U(\mathbf{r}) + \frac{1}{2}\frac{\partial U(\mathbf{r})}{\partial \mathbf{r}} + \frac{1}{8}\frac{\partial^2 U(\mathbf{r})}{\partial \mathbf{r}^2}(\delta\mathbf{r})(\delta\mathbf{r})^T\right] \tag{12}$$

The Hamiltonian for the second satellite (H_2) can be found from the preceding equation by reversing the signs of $\delta\mathbf{r}$ and $\delta\mathbf{v}$. As in the Keplerian case, H_1 and H_2 are conserved by the motion. It can be easily shown that $H_1 + H_2 = 2H$ for this generalized case.

If we now subtract the expanded H_1 and H_2 expressions, we obtain the relative Hamiltonian:

$$H_R = \mathbf{v}\cdot\delta\mathbf{v} + \frac{\partial U(\mathbf{r})}{\partial \mathbf{r}}\delta\mathbf{r} \tag{13}$$

which is simply the generalized form of Eq. (7). We can take the Hamilton's equations to obtain

$$\dot{\mathbf{r}} = \frac{\partial H_R}{\partial \delta\mathbf{v}} \qquad \dot{\mathbf{v}} = -\frac{\partial H_R}{\partial \delta\mathbf{r}} = -\frac{\partial U(\mathbf{r})}{\partial \mathbf{r}} \tag{14}$$

$$\delta\dot{\mathbf{r}} = \frac{\partial H_R}{\partial \mathbf{v}} \qquad \delta\dot{\mathbf{v}} = -\frac{\partial H_R}{\partial \mathbf{r}} = -\frac{\partial^2 U(\mathbf{r})}{\partial \mathbf{r}^2}\delta\mathbf{r} \tag{15}$$

Conservation of the relative Hamiltonian can be shown by simply substituting positions and velocities in Eqs. (14) and (15) into the time derivative of H_R, which then becomes zero.

III. Symplectic Relative Orbit Propagation

A. Numerical Integration Scheme

We have described the motion of a pair of satellites in similar orbits by describing the motion in terms of a nominal position and velocity and the relative motion between the satellites. By combining these descriptions, we can determine the position and velocity of each satellite in turn. In this section, we shall describe how both of these motions are propagated numerically. The procedure is very similar to the symplectic scheme introduced for the absolute orbit (Sec. II.A).

We will make extensive use of the Hamiltonian splitting technique, in which the Hamiltonian can be written as the sum of more than one surrogate Hamiltonian [36]. In our case, we can first split the Hamiltonian into a Keplerian part and perturbations.

Although the Keplerian motion can be modeled via analytical means (see the following section), the effects of the higher-order geopotential terms still need to be propagated numerically. Equation (3) shows the nominal velocity jump due to a nonspherical Earth. For the relative velocity jump over a full time step, we can write

$$\Delta\delta\mathbf{v} = -h\frac{\partial^2 R}{\partial \mathbf{r}^2}\delta\mathbf{r} \tag{16}$$

The numerical integration scheme described in Eq. (4) is a second-order algorithm, but it is possible to construct higher-order schemes in the following form [38]:

$$\exp(x_m hK)\exp(w_m hR)\cdots\exp(x_0 hK)\exp(w_0 hR)\exp(x_0 hK)\cdots \exp(w_m hR)\exp(x_m hK) \tag{17}$$

where $x_m = w_m/2$, $x_{m-1} = (w_m + w_{m-1})/2, \ldots, x_0 = (w_1 + w_0)/2$.

As long as the perturbations are first order, these methods will have similar orders to the error of the associated numerical integration formula. This condition is satisfied for the case of satellites orbiting the Earth, because the Keplerian potential is 10^3 times larger than the largest term in the perturbation, which is J_2. Therefore, the order of the scheme is $\mathcal{O}(J_2 h^6)$.

For the sixth-order scheme, Yoshida [35] reports that there are three solutions for w_m, but the one with smallest error is

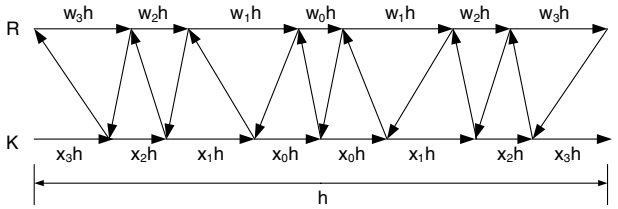

Fig. 2 Sixth-order symplectic scheme.

$$w_1 = -1.17767998417887100695$$
$$w_2 = 0.23557321335935813368$$
$$w_3 = 0.78451361047755726382 \qquad w_0 = 1 - 2(w_1 + w_2 + w_3) \tag{18}$$

Yoshida [35] obtained these solutions via numerically solving a set of three algebraic equations simultaneously. We have fully reproduced the coefficients from Leimkuhler and Reich [36], who presented higher-precision results for the same coefficients in comparison to Yoshida.

Higher-order schemes require a greater number of force calculations per integration step. In fact, the second-order scheme requires a single force calculation, whereas this increases to seven force calculations for the sixth-order scheme. Figure 2 shows how this sixth-order scheme works (compare with the leapfrog scheme, shown in Fig. 1).

The preceding sixth-order integration scheme yields accurate results, however, the force due to the higher-order geopotentials has to be computed seven times at each time step, causing a significant computational burden. Furthermore, the gains are arguably very small. The J_2 term is already an order of magnitude smaller than the two-body force field; the remaining geopotential terms are at least an order of magnitude smaller than J_2, though requiring much more complicated and lengthy calculations. The solution to this problem comes in the form of composite schemes, in which, for example, high-order integration for more significant terms can be combined with a low-order integration for higher-order terms.

Splitting the Hamiltonian further, one obtains Keplerian part K, J_2 part R_1, and the remaining geopotential terms R_2. Rewriting Eq. (4), the composite integrator is constructed:

$$\exp[\tfrac{1}{2}h(K + R_1)]\exp(hR_2)\exp[\tfrac{1}{2}h(K + R_1)] \tag{19}$$

so that the higher-order terms [denoted as $\exp(hR_{\ddagger})$] are propagated via longer time steps and a second-order scheme, whereas the more significant Keplerian and J_2 effects (denoted as $\exp[\frac{1}{2}h(K + R_1)]$) are calculated via the sixth-order scheme, saving precious processor time.

B. Keplerian Motion

Although it is possible to solve the absolute Keplerian motion numerically, the existence of an exact analytical solution can be exploited to achieve higher accuracy. For this, we use the Gauss $f - g$ functions (see [27] and Battin [39] for a particularly detailed treatment). This method is particularly appealing because it is free of singularities and does not suffer from small eccentricity effects.

To evaluate these functions we employ the Stumpff [40] c functions and introduce a set of G functions for simplicity [41]. We propagate forward in time the nominal position and velocity through the relations

$$\begin{aligned} f &= 1 - \mu G_2/r_0 \qquad g = t - \mu G_3 \qquad \dot{f} = -\mu G_1/(r_0 r) \\ \dot{g} &= 1 - \mu G_2/r \qquad \mathbf{r} = f\mathbf{r}_0 + g\mathbf{v}_0 \qquad \mathbf{v} = \dot{f}\mathbf{r}_0 + \dot{g}\mathbf{v}_0 \end{aligned} \tag{20}$$

where the position and velocity $(\mathbf{r}_0, \mathbf{v}_0)$ is at time $t - h$, where h is the time step. For the relative motion, we can compute the variational equations for f and g [32]; although these equations themselves are not novel, their use in the relative motion is novel. Note that this procedure is not exact and does cause small errors in relative motion. The variational equations for the Keplerian update can be expressed as

$$\begin{aligned} \delta f &= \mu G_2 \delta r_0/r_0^2 - \mu\delta G_2/r_0 \qquad \delta g = -\mu\delta G_3 \\ \delta\dot{f} &= -\mu\delta G_1/(r_0 r) + \mu G_1(\delta r_0/r_0 + \delta r/r)/(r r_0) \\ \delta\dot{g} &= -\mu\delta G_2/r + \mu G_2\delta r/r^2 \\ \delta\mathbf{r} &= f\delta\mathbf{r_0} + g\delta\mathbf{v_0} + \mathbf{r_0}\delta f + \mathbf{v_0}\delta g \\ \delta\mathbf{v} &= \dot{f}\delta\mathbf{r_0} + \dot{g}\delta\mathbf{v_0} + \mathbf{r_0}\delta\dot{f} + \mathbf{v_0}\delta\dot{g} \end{aligned} \tag{21}$$

This completes the Keplerian update for the nominal and relative positions and velocities. Note that we will call this the $\delta f - \delta g$ method for relative Keplerian motion.

Malhotra [26] proposed a modification to the $f - g$ functions to include a simple drag model with a force acting on the alongtrack direction. Although we have not implemented it in our propagator, this model can be easily adapted into relative drag via taking the variations. Strictly speaking, once the drag is taken into account, a numerical scheme is no longer symplectic because the system becomes dissipative.

C. Notes on Implementation

The propagator code was written in C programming language. It is initialized using a config file with inertial coordinates of the two satellites and the date, as well as some propagation parameters such as integration-step size and duration. The time system used is Universal Coordinated Time (UTC). Initial conditions defined are the Earth-centered inertial system at the true equator mean equinox at the epoch. During the calculation of the forces due to the tesseral harmonics, the conversions between the Earth-fixed rotating and inertial frames take into account the rotation of the Earth but not precession and nutation. These forces are calculated at each step and it was therefore necessary to find a balance between accuracy requirements and computational efficiency.

The user can specify which geopotential model to use (GEM10B or WGS84) and the number of terms in the axisymmetric or nonaxisymmetric model, depending on the speed and accuracy requirements of the application. Sanity checks of initial conditions and switches are also carried out in this step.

The next step is to make small adjustments to the satellite initial conditions via the H_R and L_R values calculated. This step was explained in detail in our previous publication [22].

As mentioned in the previous sections, the propagation is based on a composite symplectic numerical integration scheme. Figure 3 illustrates a simple composite leapfrog scheme, in which the Keplerian forces (K) are evaluated four times, the smaller effect of the potential J_2 (denoted as R_1) is calculated twice, and the effect of the remaining geopotential terms R_2, which has even smaller contribution to the overall motion, is calculated only once. As explained in preceding sections, the Keplerian propagation of the absolute and relative motion is handled via the analytical method described. The effect of J_2 and other geopotential terms are calculated as simple velocity jumps due to these forces.

The code gives the user the option of using a second (as in Fig. 3) or sixth-order scheme for the computation of Keplerian and J_2 forces. The remaining forces are calculated only once during a propagation time step.

The code outputs the coordinates of the midpoint satellite and the inertial and local relative positions and velocities. Because of the symplectic properties of the integrator, a crucial health check is the conservation of relative and absolute energies, which takes into account the contribution of all geopotential terms the user opted to include in the force model. Although a small oscillation in energy is to be expected, this diminishes as the integration-step size gets smaller. Note that for a nonaxisymmetric model, energy becomes a function of time, with $n-$daily oscillations of the tesseral harmonics.

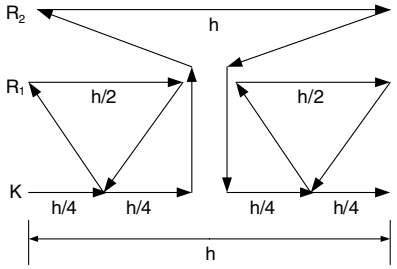

Fig. 3 Composite leapfrog symplectic scheme.

IV. Results

A. Conservation of Energy

We can show that the relative energy is an oscillation around a stable mean and that this oscillation amplitude goes to zero as the time steps get smaller. The condition for this is that the geopotential model is axisymmetric, that is, we take into account zonal harmonics only. Similarly, for such a geopotential model, the z component of the relative angular momentum is also conserved.

First, we will show that the relative energy and the z component of the relative angular momentum are zero mean oscillations. We will use an example in which we have one satellite at a 9567.2-km semimajor axis and $e = 0.3$ eccentricity and another in a similar orbit at a 23-m semimajor-axis difference in Keplerian elements. We use an axisymmetric geopotential containing terms up to J_4 only and run the propagation at 100 steps/orbit for five days (46 orbits). Figure 4 shows the variation of H_R, which is seen to be oscillating around a stable mean, with an amplitude of 4.8×10^{-11}. This shows that H_R is indeed conserved.

Second, the z component of the relative angular momentum is conserved. The variation for the preceding example compared with the initial value is just a random walk, with an error at the 10^{-16} level, which is down to machine accuracy. Therefore, conservation of the z component of the angular momentum is shown for the relative motion.

We can use this test setup to illustrate how fast the relative energy oscillation amplitude decreases as integration time steps are made smaller. We also would like to investigate whether this decrease rate is any different when compared with running two absolute propagations and taking the difference of the calculated energies. It should be emphasized that this oscillation amplitude is also an indicator of the positional accuracy. One use for this observation would be to devise an algorithm that adjusts the integration-step size according to a required accuracy level. However, this requires identifying and quantifying the effect of the parameters that change the oscillation amplitude. Therefore, this has been left for a future study.

Figure 5 shows the variation of oscillation amplitudes in H, $H_1 - H_2$, and H_R for various step sizes. As can be expected, the oscillation in H is about an order of magnitude larger than that of the relative motion. For all cases with an increasing number of steps per orbit, we can see the diminishing returns in the oscillation-amplitude decrease rate. This suggests that in practice, very small step sizes will be of limited use.

Comparing the difference in energies $H_1 - H_2$ and the relative Hamiltonian H_R, we see that their oscillation amplitudes decrease at a very similar rate, which suggests that very similar accuracies can be obtained by running the relative orbit propagator or differencing the results of two absolute propagations.

Then the question is whether we can gain CPU time for a given level of accuracy. To test this, for both the relative orbit propagation and differencing two absolute propagations, we measured processor times using the C functions `clock` and `difftime`. For consistency, each propagation was run five times and the runtimes were averaged. The execution times were around a few seconds on a computer with a AMD2400 CPU and 512 MB memory. For a geopotential model with 36 terms in the zonal and tesseral harmonics, the relative orbit propagation is found to be about 40% faster in computational time than running two absolute orbit propagations. This shows that the relative orbit scheme yields better efficiency and is ideal for applications with limited computational power.

B. Number of Geopotentials

In this section, we will compare the accuracies of geopotential models of different complexities with a high-precision geopotential model.

We will use the initial conditions given in Table 1 for a five-day propagation at 120 steps/orbit. The truth model is a 1000 steps/orbit composite symplectic scheme with a 36×36 geopotential field model; as before, we calculate the absolute orbit for each satellite with this scheme and take the difference to obtain the relative orbit.

Figure 6 summarizes the relative positioning errors after a five-day propagation with axisymmetric and nonaxisymmetric geopotential models containing various number of geopotentials. The curves labeled $H_R L_R$ and $\mathrm{d}f - \mathrm{d}g$ illustrate which method is used for the Keplerian part of the propagation (as given in Secs. II.B and III.B, respectively). The label axi shows that only an axisymmetric model is used for this run. Note that "zero geopotentials" in the figure correspond to a Keplerian force model.

Although a higher number of geopotentials increase the accuracy, as expected, excluding the tesseral terms seems to cause a large offset. The total energy difference can be written as a summation of smaller Hamiltonians due to other geopotential terms, that is, $\delta H = \delta H_K + \delta H_2 + \delta H_3 + \cdots + \delta H_{\text{tess}}$, where δH_K is the differ-

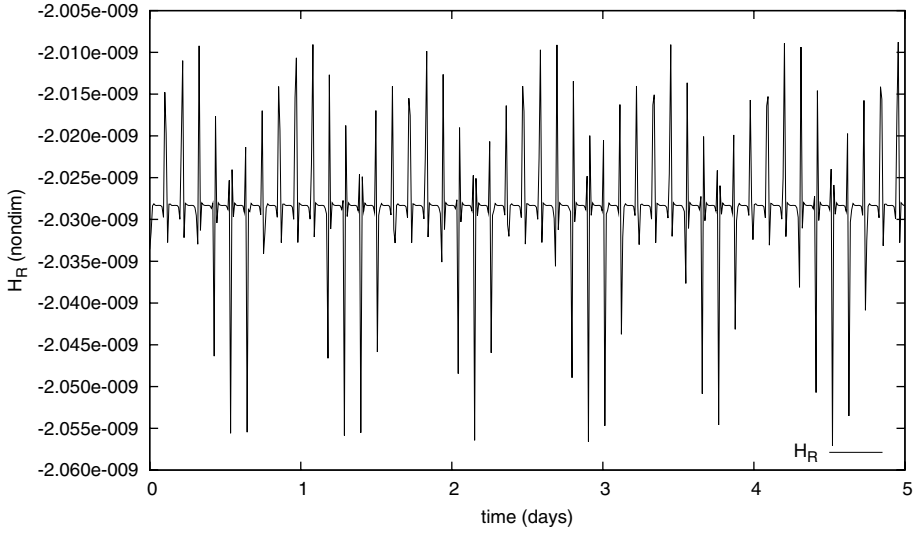

Fig. 4 Variation of the H_R with J_4 level zonal and tesseral harmonics.

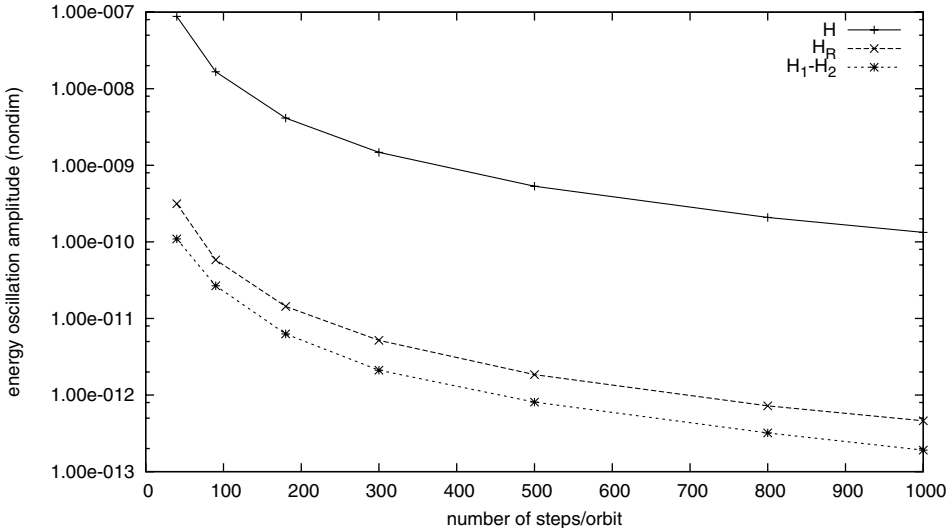

Fig. 5 Energy oscillation amplitude (log scale) in H, $H_1 - H_2$ and H_R for various integration-step sizes.

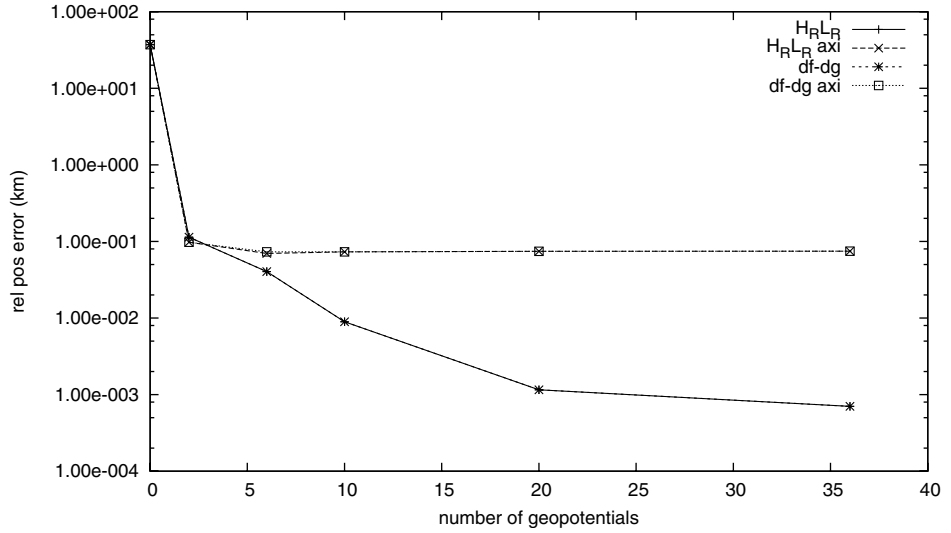

Fig. 6 Relative positioning error (log scale) with various geopotentials; five days (65 orbits).

ence in Keplerian potential, δH_2 is the difference in J_2 potential, δH_3 is due to J_3, and δH_{tess} is due to all tesseral terms. Given the coordinates of two satellites, different models will obviously yield different δH values. The energy of a satellite determines the mean motion, and the energy difference thus determines the relative mean motion or relative drift rate. Evidently, a simple model that includes four terms in the geopotential will have a significantly different drift rate with respect to a 36-term model, due to these truncated geopotential terms. As can be expected, the error in drift rate manifests itself as relative positioning errors in the alongtrack direction.

However, the most striking feature of Fig. 6 is that the $\delta f - \delta g$ and $H_R L_R$ methods yield virtually the same errors. In fact, the difference between the two methods is less than 10^{-5} m for all cases.

From these tests, we conclude that for a given set of formation initial conditions, it is possible to obtain meter-level accuracy after five days with about 20 geopotentials included in the model. More important, we showed that the two analytical methods for Keplerian relative orbit propagation are practically equivalent.

C. Relative Positioning Accuracy

We will demonstrate the relative positioning accuracy for a range of initial conditions. We also would like to show that the two relative propagation methods ($\delta f - \delta g$ method and $H_R L_R$ method presented in [22]) will yield practically the same results, because they are both first-order approximations to the relative motion.

Obviously, it is impossible to test the numerical propagator for every possible initial case. Therefore, we tried to present the cases we believe to be most representative of the overall performance of the propagator. Even then, it is not always straightforward to isolate one variable and test its effect on the accuracy. For example, suppose that we set up two satellites with similar Keplerian elements and vary a single element to investigate its effect on the motion. For a simulation

Table 1 Integration test case initial conditions in Keplerian elements

	a, km	e	I, deg	Ω, deg	ω, deg	θ, deg	H	L
Sat1	7653.780	0.0050	60.00	40.0	20.0	240.0	−0.416665	1.095432
Sat2	7653.700	0.0055	60.01	40.0	19.0	241.0	−0.416667	1.095426
Diff	−0.080	0.0005	0.010	0.0	−1.0	1.0	-2.17×10^{-6}	-5.73×10^{-6}

Table 2 Test case formation initial conditions in Keplerian elements

	a, km	e	I, deg	Ω, deg	ω, deg	θ, deg	H	L
Sat1	15,945.80	0.3500	60.00	40.03	20.00	70.00	−0.199994	1.481152
Sat2	15,945.65	0.3501	60.03	40.03	19.95	70.05	−0.199996	1.481086
Diff	−0.15	0.0001	0.030	0.030	−0.050	0.050	-1.88×10^{-6}	-6.60×10^{-5}

with perturbations to the Keplerian potential, these Keplerian elements will no longer be constant and, even if the energies in the Keplerian model are the same, the satellites will drift apart under this more complicated geopotential model. It is therefore difficult to distinguish between the errors due to increasing separation between the satellites and those due to the tested Keplerian element. Similarly, if we want to test the dependency on the semimajor axis, simply increasing it and keeping other Keplerian elements constant will not yield very useful results. The differential drift rate is proportional to H_R/H; therefore, the high semimajor cases will have much smaller separations and relative positioning errors. In short, the results need to be analyzed with due care.

The first set of tests will use the initial conditions given in Table 2 to run five-day (21.5-orbit) simulations. We will start with a Keplerian model to compare the two analytical relative orbit models. The initial separations range from 5.8 km for $e = 0.55$ to 9 km for near-circular cases. Peak separations range from 54 km for $e = 0.55$ to 34 km for near-circular cases.

Figure 7 illustrates the relative positioning error for this case through a range of eccentricities. The curves labeled $H_R L_R$ and $\mathrm{d}f - \mathrm{d}g$ illustrate which method is used for the propagation. As can be seen, the two methods yield virtually the same results, proving further that they are practically equivalent. The difference between the two remains around 10^{-7} m, regardless of the eccentricity.

The second set of tests is to repeat the preceding, but with a 36×36 geopotential model and two step sizes: 100 and 300 steps/orbit. The truth model is 1000 steps/orbit. Figure 8 shows the results for this test case, where $H_R L_R$ or $\mathrm{d}f - \mathrm{d}g$ denotes the method and 100 or 300 denotes the number of steps/orbit. As expected, the two methods yield practically identical results, with differences around 10^{-7} m or less. Although the relative positioning accuracy is very high for both the 100 and 300 steps/orbit cases, the former start to become unstable at around $e = 0.5$. For the latter, although the errors increase with eccentricity, they stay well below meter level.

We will now examine the effect of inclination on accuracy. For this, we will use the initial conditions given in Table 1, in a five-day,

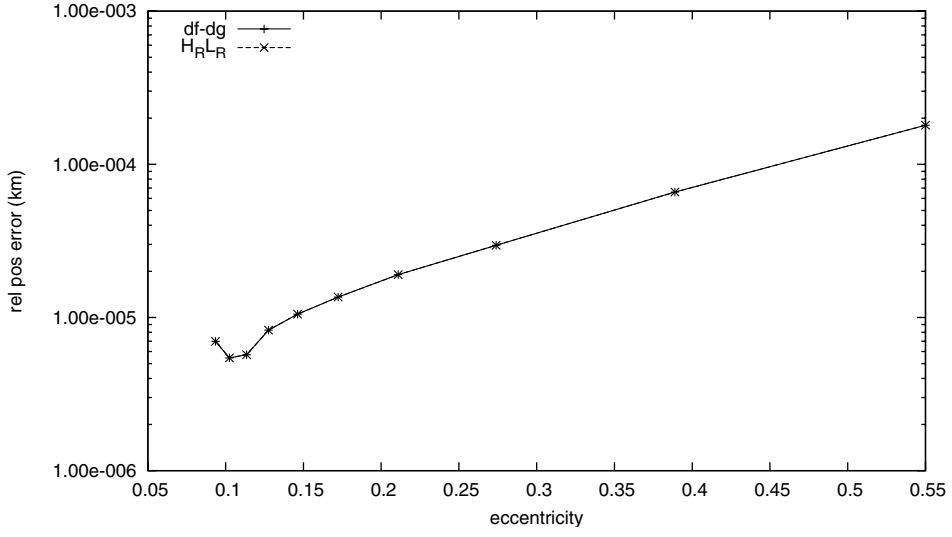

Fig. 7 Relative positioning error (log scale) with eccentricity for Keplerian potential; five days (21.5 orbits).

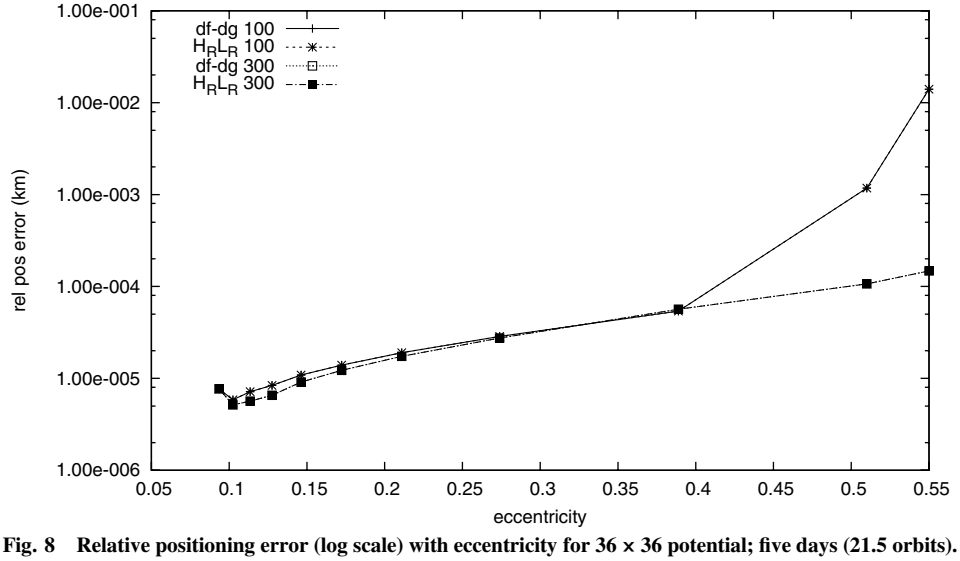

Fig. 8 Relative positioning error (log scale) with eccentricity for 36 × 36 potential; five days (21.5 orbits).

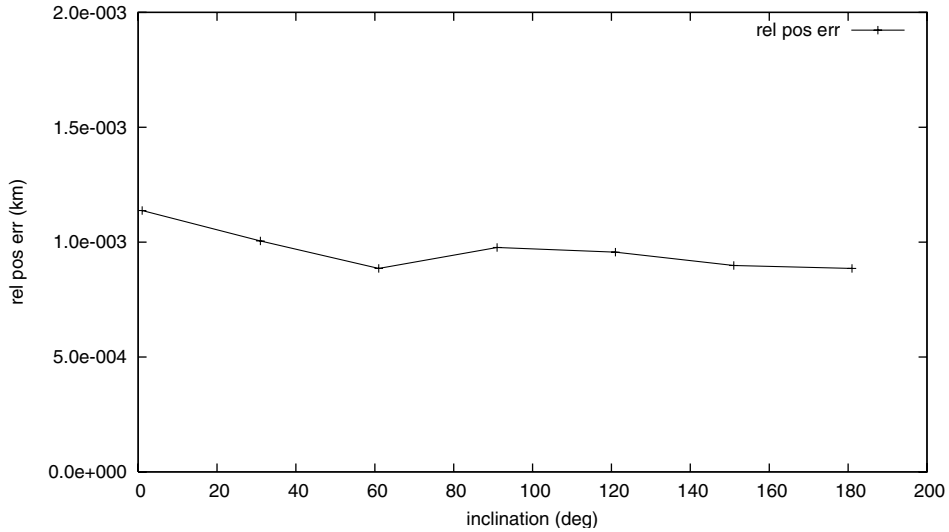

Fig. 9 Relative positioning error with eccentricity for 36 × 36 potential; five days (21.5 orbits).

36×36 geopotential model propagation with 100 steps/orbit. Among the initial Keplerian elements, only the inclination will be varied. Maximum relative positioning errors during the test runs are presented in Fig. 9.

The relative positioning errors increase linearly, to reach around the 1-m mark at the end of this five-day propagation. There is no discernible pattern in the error to suggest that inclination has a significant effect on the relative positioning error.

D. Long-Term Stability

In the preceding sections, we showed that the algorithm works remarkably well for durations of several days. However, we would like to demonstrate how it would perform when the separations are well beyond the close-proximity assumption; it is important to see how quickly the algorithm breaks down.

To this end, we used the initial conditions given in Table 1, but with a 600-m semimajor-axis difference rather than 80 m. We run a 50-day (650-orbit) propagation with a 36×36 geopotential model at a step size of 120 steps/orbit. The truth model is at 1000 steps/orbit, employing the same geopotential model. The separation starts from 1.5 km and exceeds 3640 km by the end of the simulation run.

Figure 10 shows the quadratic growth of the relative positioning error both in kilometers and as a percentage of the separation. Although the relative positioning error reaches 35 km by the end of 50 days, it corresponds to about 1% of the separation.

The errors in this example are in the alongtrack direction. Even though we take great care in matching the real energy difference when initializing the propagator, the residual relative energy error adds a small relative drift between the satellites. As the satellites drift apart, the assumption of "satellites in close proximity" breaks down and linear equations start to fail.

V. Conclusions

A novel method capable of propagating the relative motion between two satellites in formation about a geopotential model containing terms up to 36×36 was presented. This numerical scheme is simple to implement and builds upon the heritage of existing symplectic absolute orbit propagators. The relative propagation is symplectic and the Keplerian part of the motion is handled analytically using a novel implementation of the Gauss functions. A high-performance composite numerical integration scheme was also set up for better use of processing power. For a given integration-step size, this is about 40% faster than differencing two absolute orbit propagations, for the same level of accuracy.

The results demonstrate that the propagator can yield a meter level or better relative positioning accuracy after five days, even with 36 zonal and tesseral harmonics included in the geopotential model, without any limitations on eccentricity. It is therefore a significant step toward relative navigation filters with better dynamic models, requiring reduced sensor inputs.

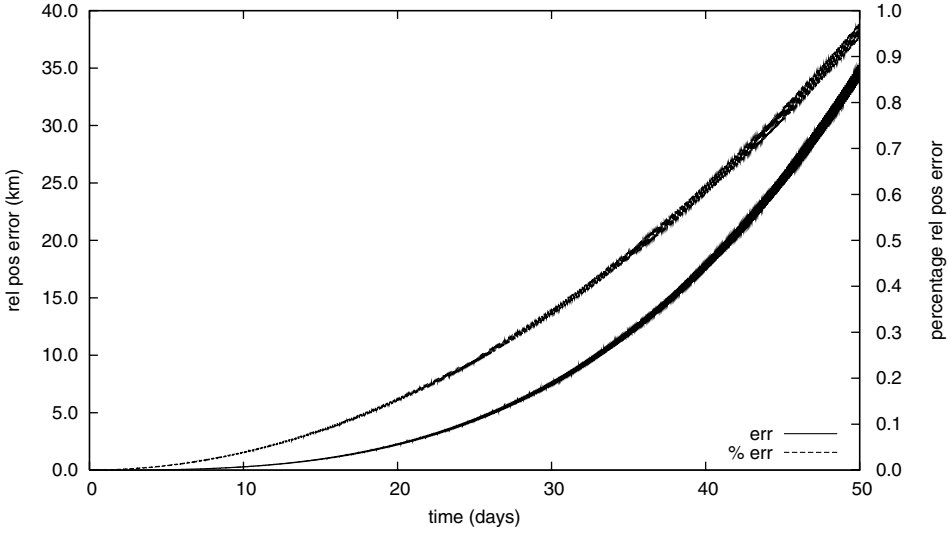

Fig. 10 Relative positioning error (log scale) in 50 days (650 orbits); percentage error is the top one.

Acknowledgments

Egemen İmre was supported by the TÜBİTAK-UZAY Space Research Institute and Surrey Space Centre throughout this work.

References

[1] Clohessy, W., and Wiltshire, R., "Terminal Guidance System for Satellite Rendezvous," *Journal of the Aerospace Sciences*, Vol. 27, No. 9, 1960, pp. 653–658, 674.

[2] Hill, G. W., "Researches in the Lunar Theory," *American Journal of Mathematics*, Vol. 1, No. 3, 1878, pp. 5–26, 129–147, 245–260.

[3] Gim, D.-W., and Alfriend, K. T., "The State Transition Matrix for Relative Motion of Formation Flying Satellites," AAS Space Flight Mechanics Meeting, San Antonio, TX, American Astronautical Society Paper 02-186, 2002.

[4] Gim, D.-W., and Alfriend, K. T., "The State Transition Matrix of Relative Motion for the Perturbed Non-Circular Reference Orbit," *Advances in the Astronautical Sciences*, Vol. 108, Jan. 2002, pp. 913–934; also American Astronautical Society Paper 01-222.

[5] Ross, M., "Linearized Dynamic Equations for Spacecraft Subject to J2 Perturbations," *Journal of Guidance, Control, and Dynamics*, Vol. 26, No. 4, 2003, pp. 657–659.

[6] Schaub, H., and Alfriend, K. T., "J_2 Invariant Relative Orbits for Spacecraft Formations," *Celestial Mechanics and Dynamical Astronomy*, Vol. 79, Feb. 2001, pp. 77–95.

[7] Schweighart, S., and Sedwick, R., "Perturbative Analysis of Geopotential Disturbances for Satellite Formation Flying," *2004 IEEE Aerospace Conference Proceedings*, Vol. 2, Inst. of Electrical and Electronics Engineers, Piscataway, NJ, 2001, pp. 1001–1019.

[8] Schweighart, S., and Sedwick, R., "High-Fidelity Linearized J_2 Model for Satellite Formation Flight," *Journal of Guidance, Control, and Dynamics*, Vol. 25, No. 6, 2002, pp. 1073–1080.

[9] Broucke, R., "Solution of the Elliptic Rendezvous Problem with the Time as Independent Variable," *Journal of Guidance, Control, and Dynamics*, Vol. 26, No. 4, 2003, pp. 615–621.

[10] Inalhan, G., Tillerson, M., and How, J., "Relative Dynamics and Control of Spacecraft Formations in Eccentric Orbits," *Journal of Guidance, Control, and Dynamics*, Vol. 25, No. 1, 2002, pp. 48–59.

[11] Lawden, D., "Fundamentals of Space Navigation," *Journal of the British Interplanetary Society*, Vol. 13, May 1954, pp. 87–101.

[12] Melton, R., "Time-Explicit Representation of Relative Motion Between Elliptical Orbits," *Journal of Guidance, Control, and Dynamics*, Vol. 23, No. 4, 2000, pp. 604–610.

[13] Tschauner, J., and Hempel, P., "Optimale Beschleunigeungsprogramme fur das Rendezvous-Manover," *Acta Astronautica*, Vol. 10, Nos. 5–6, 1964, pp. 296–307.

[14] Carter, T., and Humi, M., "Fuel-Optimal Rendezvous Near a Point in General Keplerian Orbit," *Journal of Guidance, Control, and Dynamics*, Vol. 10, No. 6, 1987, pp. 567–573.

[15] Kormos, T., "Dynamics and Control of Satellite Constellations and Formations in Low Earth Orbit," Ph.D. Thesis, Univ. of Surrey, Guildford, England, U.K., 2004.

[16] O'Donnell, K., "Satellite Orbits in Resonance with Tesseral Harmonics: Absolute and Relative Orbit Analysis," Ph.D. Thesis, Univ. of Surrey, Guildford, England, U.K., 2005.

[17] Kormos, T., and Palmer, P., "Modelling and Control of Relative Orbits for Spacecraft Flying in Formation in LEO," *Proceedings of the 3rd International Workshop on Satellite Constellations and Formation Flying*, Servizio Tecnografico Área della Ricerca Del CNR, Pisa, Italy, 2003, pp. 279–286.

[18] Wiesel, W., "Relative Satellite Motion About an Oblate Planet," *Journal of Guidance, Control, and Dynamics*, Vol. 25, No. 4, 2002, pp. 776–785.

[19] Karlgaard, C., and Lutze, F., "Second-Order Relative Motion Equations," *Journal of Guidance, Control, and Dynamics*, Vol. 26, No. 1, 2003, pp. 41–49.

[20] Melton, R., "Comparison of Relative-Motion Models for Elliptical Orbits," *Proceedings of the 3rd International Workshop on Satellite Constellations and Formation Flying*, Servizio Tecnografico Área della Ricerca Del CNR, Pisa, Italy, 2003, pp. 181–189.

[21] Alfriend, K., and Yan, H., "Evaluation and Comparison of Relative Motion Theories," *Journal of Guidance, Control, and Dynamics*, Vol. 28, No. 2, 2005, pp. 254–261.

[22] Palmer, P., and İmre, E., "Relative Motion Between Satellites on Neighbouring Keplerian Orbits," *Journal of Guidance, Control, and Dynamics*, Vol. 30, No. 2, 2007, pp. 521–528.

[23] Bate, R., Mueller, D., and White, J., *Fundamentals of Astrodynamics*, Dover, New York, 1971.

[24] Busse, F. D., Simpson, J., and How, J. P., "Demonstration of Adaptive Extended Kalman Filtering for LEO Formation Estimation Using CDGPS," *The Journal of the Institute of Navigation*, Vol. 50, No. 2, 2003, pp. 79–94.

[25] Inalhan, G., Busse, F., and How, J., "Precise Formation Flying Control of Multiple Spacecraft Using Carrier-Phase Differential GPS," *Spaceflight Mechanics 2000*, Advances in Astronautical Sciences, Vol. 105, 2000, pp. 151–167; also American Astronautical Society Paper AAS 00-109.

[26] Malhotra, R., "A Mapping Method for the Gravitational Few-Body Problem with Dissipation," *Celestial Mechanics and Dynamical Astronomy*, Vol. 60, No. 3, 1994, pp. 373–385.

[27] Vallado, D. A., *Fundamentals of Astrodynamics and Applications*, 2nd ed., Microcosm, Inc., Hawthorne, CA, 2001.

[28] Montenbruck, O., and Gill, E., *Satellite Orbits: Models, Methods and Applications*, Springer, Heidelberg, Germany, 2001.

[29] Palmer, P., Aarseth, S., Mikkola, S., and Hashida, Y., "High Precision Integration Methods for Orbit Modelling," *Journal of the Astronautical Sciences*, Vol. 46, No. 4, 1999, pp. 329–342.

[30] Kinoshita, H., and Yoshida, H. A. N. H., "Symplectic Integrators and Their Application in Dynamical Astronomy," *Celestial Mechanics and Dynamical Astronomy*, Vol. 50, No. 1, 1990, pp. 59–71.

[31] Mikkola, S., "Efficient Symplectic Integration of Satellite Orbits," *Celestial Mechanics and Dynamical Astronomy*, Vol. 74, No. 4, 1999, pp. 275–285.

[32] Mikkola, S., Palmer, P., and Hashida, Y., "A Symplectic Orbital Estimator for Direct Tracking on Satellites," *Journal of the Astronautical Sciences*, Vol. 48, No. 1, 2001, pp. 109–125.

[33] Palacios, M., "Symplectic Versus Other Propagators in the Ideal Formulation of the Earth Satellite Problem," International Symposium on Space Dynamics, Biarritz, France, Centre National d'Etudes Spatiales Paper MS00–36, 2000.

[34] Wisdom, J., and Holman, M., "Symplectic Maps for the N-Body Problem," *Astronomical Journal*, Vol. 102, Oct. 1991, pp. 2022–2029.

[35] Yoshida, H., "Construction of Higher-Order Symplectic Integrators," *Physics Letters A*, Vol. 150, Nov. 1990, pp. 262–268.

[36] Leimkuhler, B., and Reich, S., *Simulating Hamiltonian Dynamics*, Cambridge Univ. Press, Cambridge, England, U.K., 2004.

[37] Goldstein, H., Poole, C., and Safko, J., *Classical Mechanics*, 3rd ed., Addison–Wesley, Reading, MA, 2002.

[38] Mikkola, S., and Palmer, P., "Simple Derivation of Symplectic Integrators with First Order Correctors," *Celestial Mechanics and Dynamical Astronomy*, Vol. 77, Aug. 2000, pp. 305–317.

[39] Battin, R., *An Introduction to the Mathematics and Methods of Astrodynamics*, revised ed., AIAA Education Series, AIAA, Reston, VA, 1999.

[40] Stumpff, K., *Himmelsmechanik*, Band I, VEB Deutscher Verlag der Wissenschaften, Berlin, Germany, 1962.

[41] Stiefel, E. L., and Scheifele, G., *Linear and Regular Celestial Mechanics*, Springer, Berlin, Germany, 1971.